Journal of Lasers, Optics & Photonics
ISSN: 2469-410X
Kharzheev, J Laser Opt Photonics 2017, 4:1
DOI: 10.4172/2469-410X.1000148
Research Article Open Access

Scintillation Detectors in Modern High Energy Physics Experiments and Prospect of Their use in Future Experiments

Yuri Kharzheev*

Joint Institute for Nuclear Research, Dzhelepov Laboratory of Nuclear Problems, Dubna, Moscow, Russia

Abstract

The scintillation detector (SD) based on organic plastic scintillator (OPS) is one of the basic detectors in HEP experiments. Technologies for production of OPSs as strips and tiles, their optical and physical properties, light collection based on wavelength shifting (WLS) fibers coupled to multipixel vacuum and silicon PMs are presented. SDs are multifunctional: calorimeters, triggers, tracking, time-of-flight and veto systems are the examples of their applications. The use of SDs in many HEP experiments on the search for quarks, new particles and H bosons (D0, ATLAS, CMS), quark-gluon plasma (ALICE), CP violation (LHCb, KLOE), v-oscillation (MINOS, OPERA), cosmic particles (AMS-02) are discussed. SDs hold great promise for future HEP experiments due to their ability of high segmentation, WLS fiber light collection and multipixel silicon PM readout.

Keywords: Scintillation detectors; Fibers; Calorimetry; Energy

Introduction

Scintillation detectors (SDs) based on the organic plastic scintillators (OPS) are among of the basic detectors used in the majority of the High Energy Physics Experiments [1,2]. They are reliable and efficient, simple to design and operate, can be easily calibrated and monitored, take little space in the modern spectrometric facilities and meet to the large extent the requirements on the stability of its characteristics and radiation hardness. They are multifunctional; calorimetry, triggers, tracking, time-of-flight and veto systems are the main fields of their applications.

The OPS production technology is well developed in many scientific centers - bulk polymerization (worldwide), injection molding (IHEP, Protvino, Russia) and extrusion (FNAL/NICADD, USA; ISMA, Kharkov, Ukraine; Uniplast, Vladimir, Russia) allows fabricating scintillating plates (tiles) and bars (strips) of any forms and sizes in large amounts and at a relatively low cost. The length of the strips may be up to about 10 m or more. For the efficient light collection the strips are co-extruded with reflective TiO_2 and groove(s) or hole(s) for inserting wavelength shifting (WLS) fiber (Figures 1 and 2).

The signals from strips or tiles are read out by WLS fibers (usually with 2 claddings) inserted into groove(s) or hole(s) and are usually glued into them by some high optical transparent glue. The fiber readout system is compact and efficient and collects more light than traditional light guides and nowadays it is accepted concept. The signals from each strip (tile) can be fed through the fiber by internal total reflection to the individual pixels of the multianode vacuum PMT or the multipixel silicon PM.

The Efficiency of the Scintillation Detectors

The efficiency of the SD is one of its main characteristics. Very high efficiency (99.99%) of SD is required in many high energy physics experiments, for instance, for the Cosmic Veto system in Mu2e experiment [3]. The SD efficiency is determined by the light yield and collection of the "scintillation strip – WLS fiber-photo detector (PD)" system. The light yield of the scintillation strips depends on the scintillation materials (base and dopants used) and production technology. Scintillation strips (tiles) are usually fabricated with polystyrene (C_8H_8)n as a base and some fluorescent dopants (1-3)% (PPO or PTP) and wavelength shifter (0.01-0.04)% POPOP. Scintillators on the basis of the polyvinyl toluene (C_9H_{10})n produces more light yield but it is difficult for mechanical treatment of its, so they are used as tiles but not as strips. Scintillation strips are usually coextruded with a thin layer of diffusive reflective materials TiO_2 (with thickness up to 100 µm) or the surface of the strips is subjected to special chemical etching. Tiles are usually covered with high reflective materials (TYVEK, VM2000, Al foil, etc). The light collection performed by the WLS fiber depends not only on the properties of the fiber, but also on many other (external) factors, such as gluing or not gluing the fiber in the groove or the hole, mirroring or not mirroring the fiber end. Usually fiber's ends are polished using diamond polishing process and the fiber end far from PD is mirrored by Al sputtering process. As it was shown, light collection of Kuraray WSL for various dye concentration ppm has almost identical values at ppm=200 and 300, while at ppm=150 it is less than 30% [4].

In our recent work we investigated these external factors on the light collection [5]. It was shown that injecting the optical resins (CKTN-MED(E) and BC-600 without its hardeners) into the co-extruded hole of the 2-m long plastic scintillation strip of triangle cross section (base 33 mm and height 1.7 mm) improved light collection a factor of up to 1.7-1.9 against the "dry" (without resin) case under the same conditions (Figure 3). The measurements were carried out on cosmic muons.

These resins were selected for their high optical transparency and, more importantly, for their refractive indices 1.60 (CKTN-MED) and 1.57 (BC-600) are very close to that of polystyrene (1.59). However, the resins had high viscosity and were therefore injecting them into hole the special technology was developed by us [5].

***Corresponding author:** Yuri Kharzheev, Joint Institute for Nuclear Research, Dzhelepov Laboratory of Nuclear Problems, Dubna, Moscow, Russia, Tel: (496 21) 6-21-21; E-mail: kharzheev@mail.ru

Received January 17, 2017; **Accepted** January 31, 2017; **Published** February 15, 2017

Citation: Kharzheev Y (2017) Scintillation Detectors in Modern High Energy Physics Experiments and Prospect of Their use in Future Experiments. J Laser Opt Photonics 4: 148. doi: 10.4172/2469-410X.1000148

Citation: Kharzheev Y (2017) Scintillation Detectors in Modern High Energy Physics Experiments and Prospect of Their use in Future Experiments. J Laser Opt Photonics 4: 148. doi: 10.4172/2469-410X.1000148

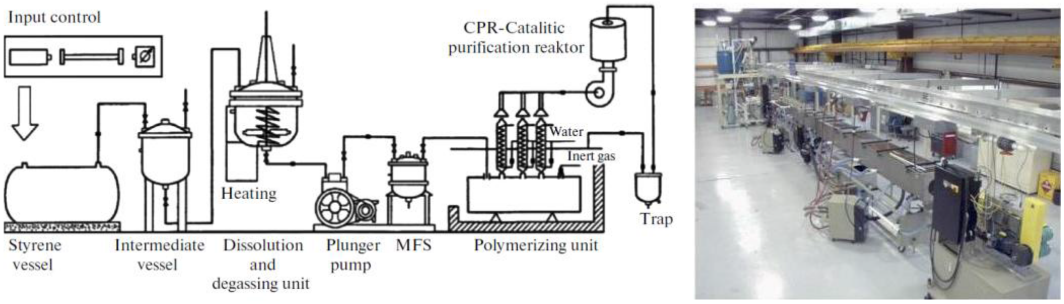

Figure 1: Schematic view of the bulk polymerization plant at ISMA (left) and a photo of the FNAL/NICADD extrusion line (right).

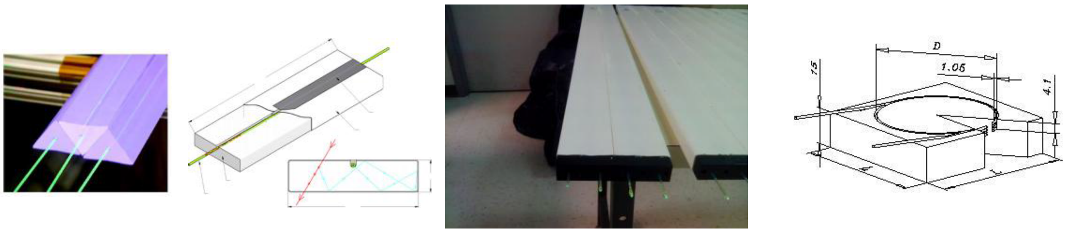

Figure 2: Strips and tile used in various experiments: a strip triangular in cross section with a hole for the WLS fiber (MINERvA, SciBar, POD T2K); a strip rectangular in cross section with a groove on its wide side (MINOS, OPERA, T2K), two strips glued together (di-counter) with two holes in each (Mu2e) and a tile with deep groove (LHCb).

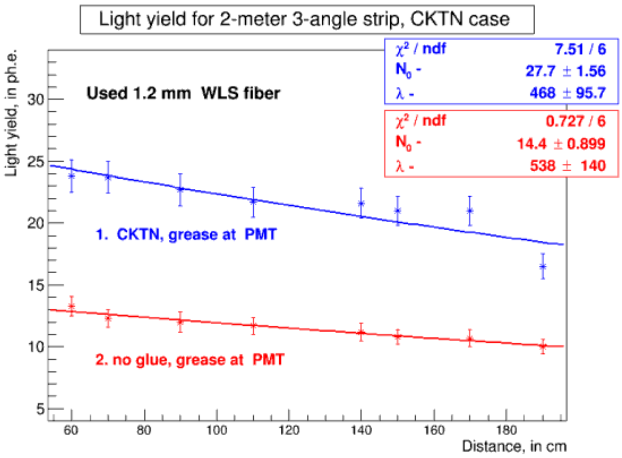

Figure 3: Light yield from cosmic muons as a function of the distance from PD for the strip filled by CKTN-MED (E) resin (curve 1) and without this resin (curve 2). Readout was performed by the 1.2-mm WLS fiber coupled to PMT with optical grease in both cases.

Similar improvement in light collection (1.7) was observed in the measurements carried out on 5-m long strip having the same cross section and CKTN-MED filler in the strip hole as in the 2-m strip case. The strip was irradiated by radioactive sources Co^{60} and Sr^{90} and its light yield (PMT anode current) was measured by Keithley 6487 picoammeter as a function of distances from PMT [6].

One of the main parameter of PD is its quantum efficiency (QE). For the wavelength $\lambda \geq 500$ nm the QE is about: 20% for vacuum PMT with bialkali cathode, (30-50)% for the SiPM and 90% for the APD (see below section Photo detectors).

Fibers in the Tracking Systems

Scintillating fibers (SciFi) and WLS fibers were used for tracking

Figure 4: A photograph of a single plane of SciFis coupled to OptFis on both sides.

in many experiments. The central tracking system of the DO-II experiment comprised a silicon microstrip and fiber trackers [6]. The fiber tracker was consisted of 8 cylindrical fiber layers (Kuraray double-clad WLS fibers 835 μm in diameter) mounted at 20 cm (innermost) to 52 cm (outermost) from beam in the radial direction. Both central trackers determined primary interaction vertex with a resolution of about 35 μm.

The ALFA detector of the ATLAS spectrometer for LHC luminosity measurements using protons elastic scattering at μrad angles is another example where high spatial resolution (30 μm) was obtained. Kuraray SCSF-78 square (0.5 × 0.5 mm) single cladding S-type fibers were used. Very small cross talk between the adjacent fibers (1.5%) was achieved by coating fiber surfaces with vacuum evaporated Al film about 100 nm thicknesses [7].

Scintillating fiber beam hodoscope comprised of 2 mm round SCSF-78M was used for discrimination of muons and electrons in a mixed-particle beam for the MUSE experiment at PSI (Figure 4). Identification of the particles based on time-of-flight technique was efficiently realized [8].

Calorimetry

One of the main fields of using SDs in HEP is calorimetry for measuring energy depositions and coordinates of particles and showers and for triggering some particular events. At the energies ~ 1TeV absorbers with thickness about 30 X_0 (18 cm Pb) or 11 nuclear lengths (2 m Fe) are needed to absorb the full energy of the electromagnetic (e/m) or hadronic showers, respectively. The transverse dimensions of the e/m calorimeters and the size of its cells, are defined by the Moliere radius R_M, a radius of an infinitely long cylinder within which 95% of the shower energy is concentrated [9,10].

R_M (g/cm^2) $\approx 21X_0/E_c$, where E_c is the critical energy in MeV, X_0 is radiation length in cm.

The calorimeter system of the modern large spectrometer comprises of electromagnetic calorimeter (ECAL) followed by hadronic calorimeter (HCAL) preceded both by preshower detectors (PSD). OPS are used as an active absorber in all of them. Energy, time, and spatial resolutions are usually described by the formula:

$a/\sqrt{E} \oplus b/E \oplus c$,

where a, b, and c are the stochastic, noise, and constant terms respectively, the sigh $\oplus$ hereafter means quadratic addition of the all terms.

The PSD usually consists of 2 layers high segmented active absorbers with a layer of passive absorber (Fe or Pb) with thickness about $2X_0$ placed between them. The PSD separates electrons from γ before they hit the ECAL and discriminating between single γ and γ of π^0 mesons decays and between π^0 π^- meson from electron. Thus the PSD in combination with ECAL are used as the trigger to indicate e, γ and π^0, π^- mesons. See for example, Central Preshower detector of D0-II detector [6] (Figure 5).

Sandwich hadronic calorimeters

The Sandwich type hadronic calorimeters are used in many experiments Akchurin and Wigmans [11], Chatrchyan et al. [12], Shopper [13]. A bright example of the sandwich calorimeter, comprised of alternating steel plates (14 mm) and scintillation tiles (3 mm), is the Hadron Tile Calorimeter of the ATLAS spectrometer with a total length of about 11 nuclear units (Figure 5, centre)) [9]. 460 000 tiles were made from polystyrene with dopants (1.5% PPO and 0.044% POPOP) using the injection molding technique [14]. Rigorous requirements were imposed on the geometrical parameters of the tiles (<0.1 mm), and smoothness and planarity of the tile surfaces (better than 20 µm). The segmentation of calorimeter in Δη (pseudo rapidity) and Δφ (azimuthally angle) was 0.1 × 0.1 (which is small than characteristic transverse dimensions of showers) and allowed the coordinators of jets to be measured with a good accuracy. The energy resolution of the tile calorimeter was described by the formula [11] (Figure 5).

$\sigma E/E = (52.9 \pm 0.9)\%/\sqrt{E} \oplus (5.7 \pm 0.2)\%$

Shashlik type calorimeters

Shashlik type calorimeters are used as the electromagnetic calorimeters (ECAL), comprised of alternating scintillation tiles (cells) and lead plates with perforated holes for setting WLS fibers. A typical feature of such a calorimeter is its high homogeneity and time resolution, radiation hardness and reliable operation. Depending on the cell size and the distances between the holes one can have different segmentation of the calorimeters and thus different energy and space resolutions.

LHCb ECAL consisted of 67 planes of scintillation tiles (4 mm thick) and 66 lead planes (2 mm thick) (Figure 5 right). Distances between the holes are 10.1 mm. Total radiation length and Moliere radius are 25 X_0 and 3.5 cm respectively. The energy resolution of the calorimeter is described by the formula [13]:

$\sigma E/E \sim 9\ \%/\sqrt{E} \oplus 0.8\%$.

A similar ECAL was used in many experiments: ALICE [15], KOPIO [16], COMPASS-II [17] et al. The ALICE ECAL was intended for measuring electromagnetic showers of e and γ with momentum up to 250 GeV/c and served as an efficient trigger for showers of e/γ and γ/π and also e/h discrimination. The modules consisting of 2 × 2 optically isolated towers was built from 76 layers of Pb plates (1.44 mm thick) interleaved with 77 layers of tiles (1.77 mm thick) with (ΔηxΔφ=0.014 × 0.014). The detector thickness was about 20 X_0. As it operated in a strong magnetic field the Hamamatsu APD S8664-55, non-sensible to magnetic field, were used. The light was collected by Kuraray Y11(200)MC WLS fibers. The test of the prototype modules showed that the energy and position resolutions were described by the formula [15]:

$\sigma E/E$, $\% = (1.7 \pm 0.3) \oplus (11.1 \pm 0.4)/\sqrt{E} \oplus (5.1 \pm 0.7)/E)$ and σx, mm=$1.5 \oplus 5.3/\sqrt{E}$, E is in GeV.

Excellent energy and time resolutions were obtained in the KOPIO detector due to the light collection non-uniformity of the tiles less than 3% and the use of API 630-70-74-510 with very high quantum efficiency of 94%:

$\sigma E/E, \% = (1.96 \pm 0.1) \oplus (2.74 \pm 0.05)/\sqrt{E}$ and

σt, ps$= (72 \pm 4)/\sqrt{E} \oplus (14 \pm 2)/E$, where E is in GeV

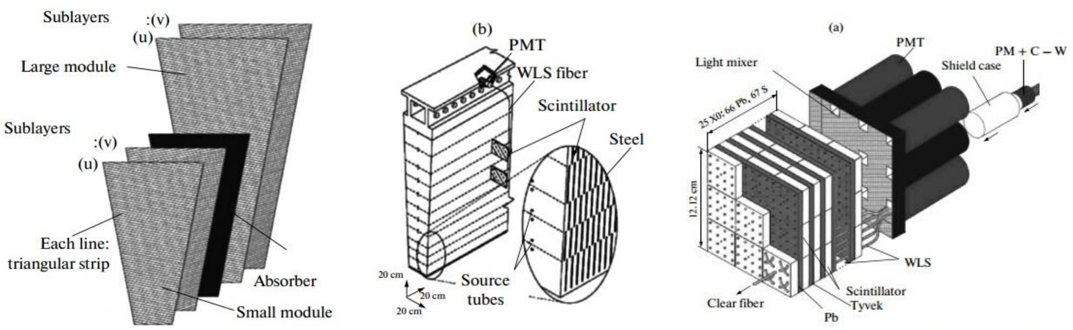

Figure 5: Schematic view of the Central Preshower detector of D0-II (left), ATLAS tile calorimeter module (centre) and LHCb ECAL (right).

The spaghetti-type calorimeters

The spaghetti-type calorimeters are the fastest, smallest-sized and radiation hardest e/m calorimeters where the passive elements are Pb plates (foils) with round grooves in which fibers are glued as active elements. The KLOE ECAL [18] is one of these type calorimeters (Figure 6).

It was designed for the studying CP violation in the decay of neutral kaons. Each module consists of a stack of 200 grooved Pb plates (foils) 0.5 mm thick and 200 layers of 1 mm-diameter Kuraray SCFI-81 fibers in the inner parts and Pol.Hi.Tech.0046 fibers in the outer parts of the calorimeters (Figure 6a). The fibers were glued into the grooves. The foil thickness was maintained to an accuracy of a few microns and the straightness of the grooves was kept at a level of 0.1 μm over a length of 1 m. The machined ends of the module and lead-fiber matrix are shown on Figures 6b and 6c, respectively. The module was read out by the light guides coupled to the fine-mesh Hamamatsu R5946/01. The energy and time resolutions were described by formulas:

$\sigma E/E$, %=5.7/√E (with a negligible constant term) and σt, ps=54/√E ⊕140, where E is in GeV.

The prototype ECAL for the (g-2) experiment is a tungsten-fiber electromagnetic calorimeter, quite compact, super dense, and easy for manufacture [19]. It consists of thin (500 μm) W plates and 500 μm BCF-10 fibers arranged into ribbon (Figure 7a). The plates and the fibers are glued together to make a rigid module 4 × 4 × 11 cm (Figure 7b). 20 modules make up an assembly (Figure 7c). The radiation length and Molière radius were 0.69 cm and 1.73 cm, respectively. The measured value of the stochastic term in the formula for energy resolution (in the energy range of 1.5-3.5 GeV) was 11.1 ± 0.4).

The Space Experiment AMS-02

The space experiment AMS-02 [20-23] is a detector that implements modern technological advances in experimental high-energy physics (Figure 8). It can identify cosmic leptons and nuclei in wide energy range from hundred MeV to few TeV per nucleon with an unprecedented accuracy.

The electromagnetic calorimeter of its is the spaghetti-type lead-fiber ECAL made of 11 superlayers of lead foils with grooves in which SciFi fiber 1 mm in diameter are glued with epoxy. The total length of the ECAL is 17 X_0. The arrangement of the fibers in the adjacent layers was mutually orthogonal which allowed measuring X and Y coordinates of the passing particles. The light was collected by the R7600-00-M04 PMT. The measured energy resolution in the electron and proton beam tests at energies of 6-250 GeV at CERN was expressed by the formula [21]:

$\sigma E/E$,%=(10.4 ± 0.2) /√E ⊕ (1.4 ± 0.1), where E in GeV

Time-of-flight (TOF) system of the AMS-02 spectrometer [22] consisted of two upper and two lower scintillation planes of polyvinyl bars read out by fine-mesh R5948 PMT. The PMT had a high gain (10^6), good time characteristic (time rise 1.9 ns), and the capability of withstanding the magnetic field. The system allows time of flight of particles to be measured with an accuracy of ~ 150 ps and serves as a trigger for discriminating between electrons (positrons) and protons (antiprotons) up to momenta of 0.5 GeV/c to 1.5 GeV/c. The combined results of the measurements from the TOF, tracking system, and Cherenkov counter allow determination of the mass of the particles. The calorimeter is capable of discriminating protons from e^+ and antiprotons from e^- at the level up to 10^6. The new results obtained from the lepton data for 1-500 GeV indicate that there are new sources of cosmic leptons [23].

Scintillation Detectors in the Neutrino Experiments

Scintillation detectors based on the long OPS strips found wide use in many neutrino experiments (MINOS [23], OPERA [24], MINERvA [25], T2K [26] et al.) and also will be used in Mu2e [3] due to their good optical characteristics, relatively low cost, manufacturability,

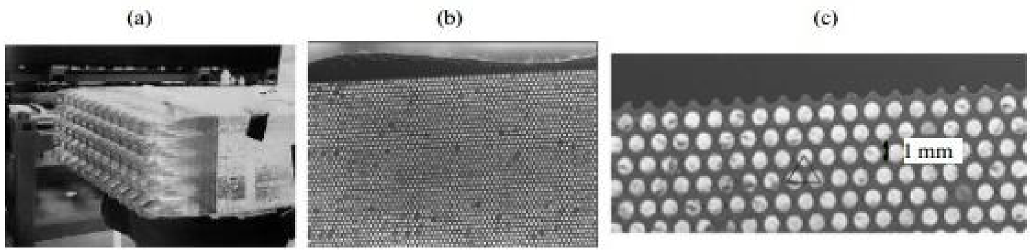

Figure 6: A photograph of a Barrel module of the KLOE ECAL equipped with light guides (a), the end of a machined module before the addition of the light guides (b), and a close-up of the fine grained matrix of scintillating fibers nested between corrugated Pb plates (c).

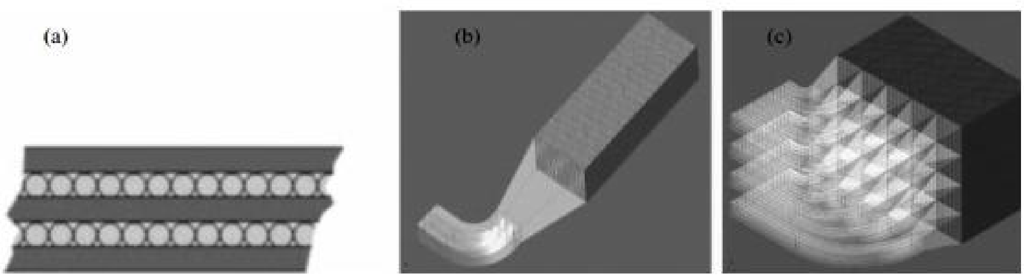

Figure 7: Tungsten plates with SciFi fibers (a), module with the light guide (b) and an assembly of 20 modules (c).

Citation: Kharzheev Y (2017) Scintillation Detectors in Modern High Energy Physics Experiments and Prospect of Their use in Future Experiments. J Laser Opt Photonics 4: 148. doi: 10.4172/2469-410X.1000148

reliable operation, ability to cover large experimental area (28 000 m^2 in MINOS), high segmentation, long term stability of characteristics, and simple calibration and monitoring procedures.

MINOS neutrino detector

The MINOS neutrino detector [23] is a sandwich-type calorimeter designed for the investigating oscillations of the muon neutrinos produced by the 120 GeV proton beam of the Fermilab Main Injectors. It consists of two similar detectors. One of them (smaller one – near detector) is located at Fermilab and the other (larger one - far detector) in the 750-m-deep Soudan mine at a distance of 735 km from near detector (Figure 9). A comparison of the number, spectra, and energies of the events in both detectors allowed the oscillation parameters to be calculated.

The detectors are comprised of the alternating magnetized steel plates (2.54 cm) and the scintillation strips (1 cm) forming 644 planes of 105 000 strips in total (Figure 9a). The planes of 192 strips were grouped into 8 modules (Figure 9b). The strips with the length up to 8 m had a rectangular form 1 cm × 4 cm with the groove (Figure 2b) in which a Kuraray Y11 (175) non-S type multiclad WLS fiber 1.2-mm in diameter was inserted. For the efficient light collection and transmission it to the PMT the WLS fibers were glued into the groove of the strip and their ends were connected with the PMT through the clear fibers (Figure 9c). The tracking system of the detector allows selecting and identifying events with charged leptons of interest (Figures 9a-c).

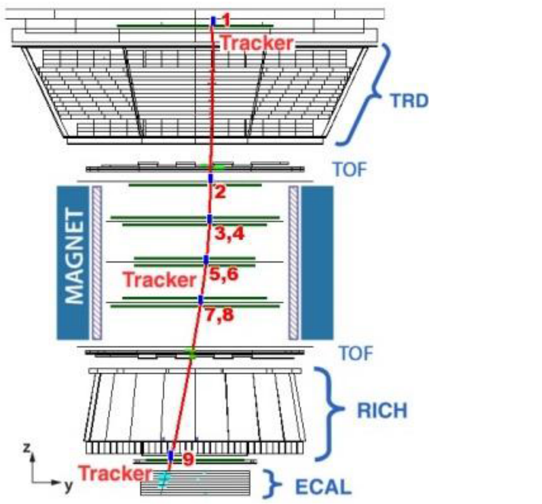

Figure 8: Schematic Y-Z view of the AMS-02 detector illustrating the path of a typical CR particle crossing various detector elements: 9 planes of the Silicon Tracker, the Transition Radiation Detector, 4 planes of the TOF Counters, the permanent magnet, the RICH counter, and the ECAL.

The light was detected by Hamamatsu R5900-00 PMT with 16 anodes and 4 × 4 mm^2 pixels for the far detector and 64 anodes and 2 × 2 mm^2 pixels for the near detector. The measured energy resolution for the electromagnetic and hadronic showers was 21.4%/√E ⊕ 4%/E and 56%/√E ⊕ 2%, respectively, and the time resolution of the far and near detectors was 2.3 ns and 5 ns, respectively [23].

OPERA detector

The OPERA detector [24] is designed to investigate neutrino oscillation ν_μ to ν_τ. It is located in the Gran Sasso underground laboratory at a distance of 730 km from CERN. The detector consists of a magnetic spectrometer and two super modules: Pb/emulsion walls and scintillation walls. Each scintillation wall was made up of 2 planes of the scintillation strips arranged in the transverse geometry (Figure 10a) for measuring X, Y coordinates of events of interest. Each plane comprises of four 6.7 × 1.66 m^2 modules consisting of 64 strips 1 × 2.6 × 670 cm^3 in size fabricated at ISMA. Charged particles in emulsion revealed a track which would be visible after the development of the emulsion.

The light was collected by Kuraray Y11(175)MC non-S WLS fibers glued into the strip's groove and transmitted to the 64-channel H7546 PMT (Figure 10b). The LED calibration of the strip allowed operation of all channel to be controlled. The signals produced in the strip were read out from both ends of the fibers, and at the centre of the strip they were equivalent 8 photoelectrons (Figures 10a and 10b).

Photo detectors

Photo detectors (PD) are components of the scintillation detectors responsible for its most importing characteristics such as light collection, energy, time and spatial resolutions. Further development and use of them in the current and future experiments substantially depend on the state and improvements of the PD properties. So, the following requirements are imposed on PDs:

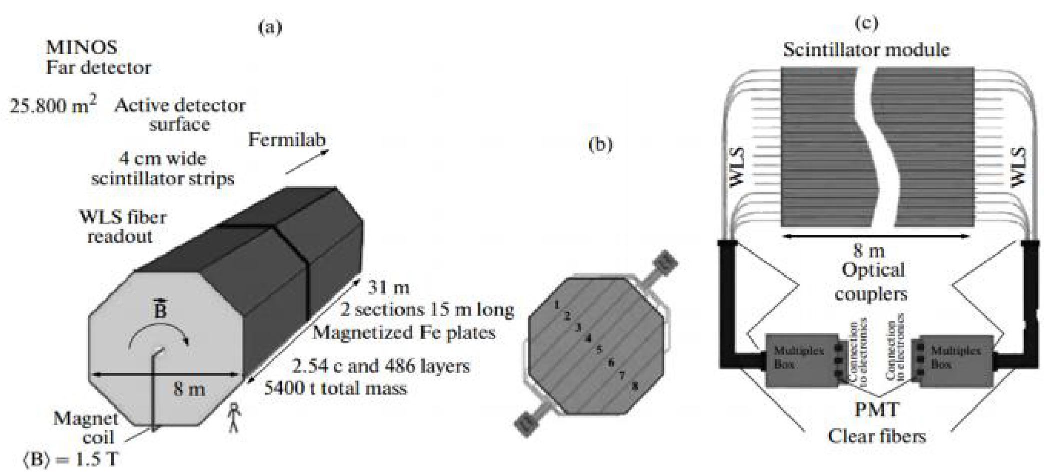

Figure 9: Schematic view of the MINOS far detector (a), a scintillation plane with 8 modules (b), and the scintillation strip readout scheme (c).

- Higher sensitivity, because light yield of long strip or small tiles can be only few photoelectrons;
- Higher uniformity of light collection and stability of characteristics;
- Compactness (ratio between the useful area of the cathode and its total area);
- Higher pixelization, which is necessary for fiber readout of signals from strip and tiles;
- Better ability to withstand strong magnetic field and radiation;
- Low cost and smaller size.

Multianode PMTs (MA PMTs): Multianode PMTs (MA PMTs) are widely used in modern SDs due to their high gain (10^6), high resolution of single photon registration, and segmentation of their anodes. Some examples of them are R7877 (ATLAS), R5900 (AMS-02), R7546 (OPERA), R7899 (LHCb ECAL). Their disadvantages are high voltage of supply and inability to operate in a magnetic field without special antimagnetic shielding, low compactness and low quantum efficiency (about 20% in visible light region).

Hybrid avalanche photodiodes (HAPD): Hybrid avalanche photodiodes (HAPD) combine advantages of PMTs (high sensitivity) and semiconductor PDs (high spatial and energy resolution, insensibility to magnetic field and simplicity of manufacture and segmentation). However, high supply voltage, and higher temperature and voltage stabilization are needed for the reliable operation of HAPD.

Avalanche photodiodes (APDs): Avalanche photodiodes (APDs) has the QE higher than 70% in the visible region. They are insensitive to the magnetic field and but their gain is no higher than 10^4 due to breakdown as in HAPD. Hamamatsu S8141 APD used In the CMS ECAL had the QE more than 80% in the visible region (Figure 11) [27].

Limited Geiger mode avalanche photodiodes: Limited Geiger mode avalanche photodiodes (SiPM or G-APD) are matrices of a lot of independent APDs with size of 30 × 30 (50 × 50, 100 × 100) μm^2 connected by a common bus to which a bias voltage 10 to 15 % higher than the breakdown voltage is applied. SiPMs are highly sensitive to single photons and have a gain of 10^6 to 10^7, and are insensitive to the magnetic field, have low power consumption, and they are compact.

The QE of the SiPM (G-APD) is higher than that of the PMT but lower than that of the APD. The QE of the SiPM p-type (optimal for green-red light detection) and n-type (optimal for blue-UV light detection) are presented on Figures 12a and 12b, respectively [28].

The first detector, where the SiPM (MPPC, Hamamatsu) was used in a great number (60 000), was the ND 280 detector of the T2K neutrino experiment [26].

There are some problems in using SiPMs: dark current, crosstalk, small size of APD cells, temperature dependence of the gain, etc. Over the past years, extensive investigations have been carried out with a view to solving these problems. The MEPhI group in cooperation with the Exelites Company developed 1 × 1 mm^2 and 3 × 3 mm^2 n-type SIPMs with 50 × 50 μm^2 and 100 × 100 μm^2 pixels, respectively. The measured values of the optical crosstalk (CT) and excess noise factor (ENF) at the overvoltage up to 4 V were no higher than 3-5% and 1.02, respectively [29].

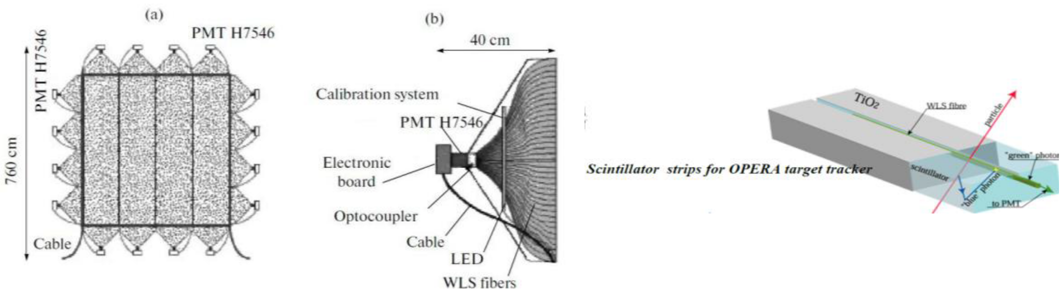

Figure 10: Schematic view of the scintillation wall with the 64-channel H7546 PMT (a), connection of the WLS fibers to the 64-channel H7546 PMT (b), and scintillation strip (right).

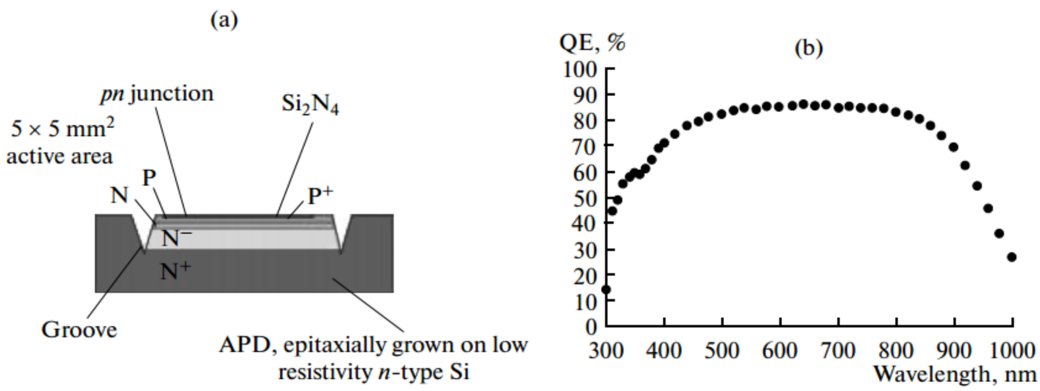

Figure 11: Structure of the Hamamatsu S8141 APD for the CMS ECAL (a) and quantum efficiency (QE) of the photodiode as a function of the wavelength (b).

Citation: Kharzheev Y (2017) Scintillation Detectors in Modern High Energy Physics Experiments and Prospect of Their use in Future Experiments. J Laser Opt Photonics 4: 148. doi: 10.4172/2469-410X.1000148

Scintillation Detectors with SiPM for Future Experiments

The requirements imposed on the detectors planned to be used at the incoming accelerators (International Linear Collider, FAIR, NICA) are very stringent. Particles will be identified by new method, PFA (Particle Flow Algorithm), which means individual identification of all shower particles, both charged and neutral, with the energy resolution better than 30%/√E. This requires very high segmentation of the calorimeter (3 × 3 cm^2 and smaller).

Prototype of analog hadron calorimeter (AHCAL) for CALICE was constructed as 38-layers sandwich calorimeter. The tiles had thick 0.5 cm and sizes 3 × 3, 6 × 6, 12 × 12 cm^2 and steel had thick 2 cm.

Light was collected by WLS fiber inserted in the tile's groove and read out by SiPM manufactured by MEPhI/PULSAR (Russia). It was shown the possibility of using the same technique for the ILC [30].

Another AHCAL with thinner tiles (0.3 cm) and new light collection method was developed [31]. Single calorimeter tile and a calorimeter module comprising 36 × 36 tiles are shown in Figure 13 (left). The tile directly coupled to the SiPM (Kuraray MCCP25-P) mounted in a special depression without a WLS fiber was tested (Figure 13b, left)). This light collection showed a high uniformity (Figures 13a and 13b).

A segmented sandwich prototype of the CALICE ECAL was developed [32]. It consisted of 26 pairs of 3-mm scintillator (Kuraray SCSN38) and a 3.5-mm absorber (82% W, 13% Co and 5% C) layers. Each scintillator layer consisted of two 45 × 90 mm^2 mega strips with nine 45 × 90 mm^2 strips with hole (F-type strip)/without hole (D-type strip) for WLS fiber (Figure 14). The total radiation length and the Molier radius were 5.3 mm and 22 mm, respectively. Strips in neighboring layers were arranged orthogonally providing high segmentation (10 × 10 mm^2) in measurement of (X, Y) coordinates. Two readout methods were realized: in the type-F signals were transmitted to the PD through the 1-mm-diameter Kuraray WLS fiber and in type-D signals were directly transmitted to the PD (strips had no holes and WLS fiber was not used). In both cases the 1 × 1 mm^2 Kuraray MPPC was used.

The use of WLS fiber increases response uniformity along the strip length but makes strip manufacture and assembly more complex. The beam test of the prototype revealed good energy resolution: the stochastic term was about 13%, and the constant term was between 3% and 4.5%, which meets the requirements for shower energy reconstruction by PFA methods.

Sandwich type ECAL (ECAL0) was developed at JINR for COMPASS-II detector at CERN. Each module of it consisted of 109 layers of alternating Pb plates and scintillating tiles with perforated holes for 1.2 mm BSF-91A WLS fibers and read out by MAPD-3N (multpixel avalanche photodiodes). The total radiation length of the module was about 15 X_0 [17] (Figure 15).

Each layer comprised of 0.8 × 119.9 × 109.8 mm^3 Pb plate and nine 1.5 × 39.95 × 39.95 mm^3 scintillation tiles making up 9 independent towers. The energy resolution was described by

$$\sigma E/E \sim 7.8\%/\sqrt{E} \oplus 2.3\%.$$

Similar modules are planned for ECAL of the multipurpose detector MPD at NICA (JINR) [33].

The development Fermilab extruded scintillator facility has shown the possibility to fabricate the scintillator strips on the unprecendented scale 35 kT for possible detector (Totally Active Scintillator Detector) in future Neutrino Factory. The planned strips may have triangular

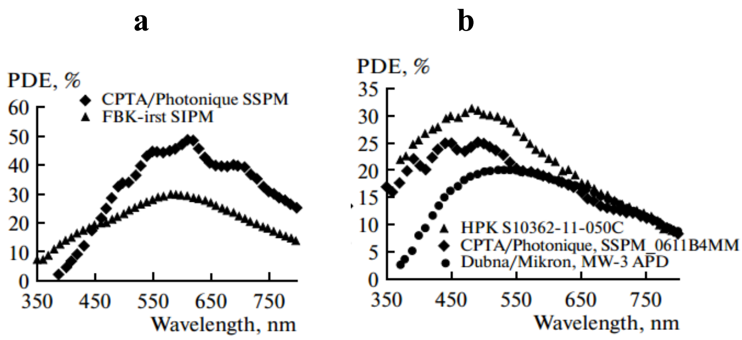

Figure 12: Photon detection efficiency as a function of the wavelength of light for the p-type CPTA/Photonique (U=42V) and FBK-irst (U=35.5V) G-APD (a) and for the n-type Hamamatsu (U=70.3V), CPTA/Photonique (U=36V) and Dubna/Micron(U=119.6V) G-APD (b).

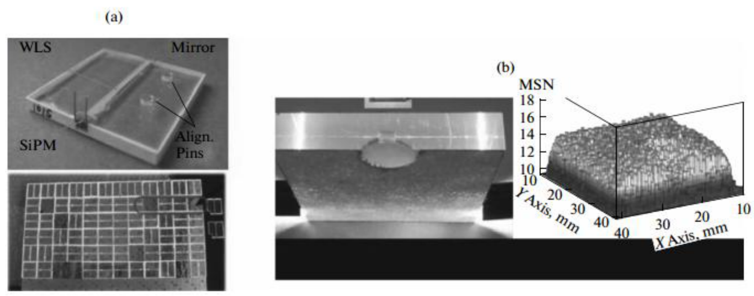

Figure 13: Single calorimeter tile (a, top) and a calorimeter module comprising 36x36 tiles (a, bottom), a single tile with a special depression for mounting the Kuraray MCCP25-P (b, left) and distribution of the signal amplitudes measured over tile surface (b, right).

Citation: Kharzheev Y (2017) Scintillation Detectors in Modern High Energy Physics Experiments and Prospect of Their use in Future Experiments. J Laser Opt Photonics 4: 148. doi: 10.4172/2469-410X.1000148

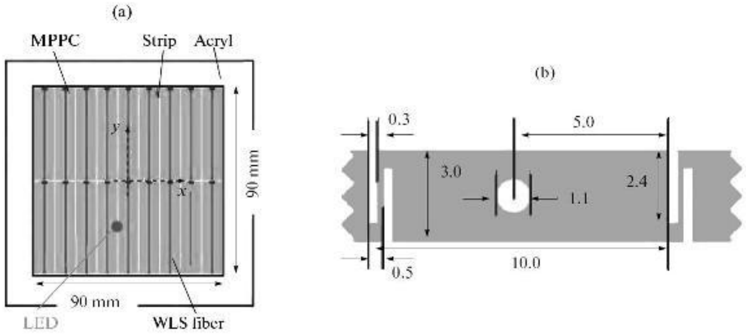

Figure 14: Structure of a type-F detector layer of the CALICE ECAL prototype (a) and the cross section of a type-F strip (b) (type-D is the same except that it has no holes, dimensions are giving in mm).

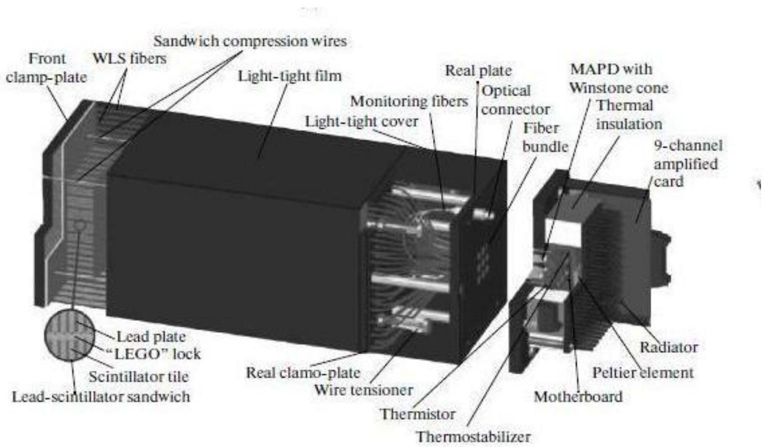

Figure 15: Scheme of ECAL0 - compact and highly segmented Shashlyk type ECAL developed at JINR for COMPASS-II detector at CERN.

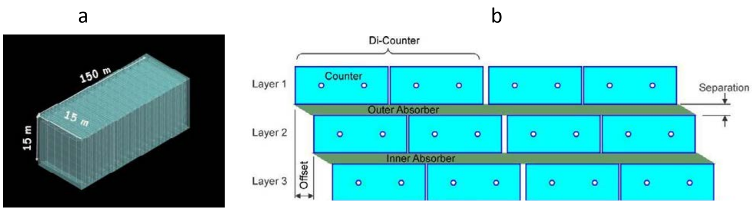

Figure 16: Schematic of the Totally Active Scintillator Detector (a) and CRV modular of Mu2e detector (b).

cross section with base 3 cm and height 1.5 cm, and length 15 m (Figure 16) [34].

The experiment Mu2e are planned at Fermilab for investigating very rare processes of conversion μ mesons into an electrons without neutrino [3]. It will be performed by the measurements 4 order better than the current limits. It's necessary to eliminate background cosmic μ mesons (which may decays into the electrons) with very high reliability. The Cosmic Ray Veto (CRV) system, covering large experimental area around Detector and partly Target solenoids, will be used. CRV will be comprises of 3(4) layers overlapping long scintillation strips read out by 1.4-mm-diameter Kuraray WLS fibers and SPMs. The required efficiency of the system is about 99.99%.

The excellent time resolution was achieved on fast scintillators with readout by SiPM. Very high single photon time resolution of 18ps/√E $MeV^{0.5}$ was obtained for small counters 3 × 3 × 2 cm^3 made of an ultrafast BC-422 scintillators and Hamamatsu MPPC S10362-33-050 efficient in near UV region [35].

Large-sized counters are often needed in HEP experiments. Counters made of ultrafast BC418, BC420, BC 422, and BC 422Q with dimensions of 60 × 30 × 5 mm^3 and 120 × 40 × 5 mm^3 were investigated [36]. HAMAMATSU, KETEK, AdvanSiD, and Sensl 3 × 3 mm^2 SiPMs with high QE in the near ultraviolet region were used for readout. The best single-photon time resolution 42 ± 2 ps per 1 MeV energy loss was obtained for counters made up of the BC-422 and a Hamamatsu HPK SiPM [37,38].

Conclusions

The importance of the SDs for modern high energy physics and astrophysics experiments can hardly be overestimated. The SDs are successfully used in calorimetry, tracking, triggering, and veto and TOF systems.

The well-developed technology for production of plastic scintillators allows fabricating scintillation tiles and strips of any form and size, and at a relatively low cost. Their optical characteristic (light yield, long-time stability, radiation hardness) meet the most requirements of modern experiments.

The prospects for the use of SDs in future experiments are closely connected with the possibility of their high segmentation and the use of fibers for collection and transmission of signals to be read out by photo detectors with a multipixel structure as SiPMs having a similar gain and higher QE than the vacuum PMT, and capability of operating in high magnetic field.

Acknowledgements

I want to thank my colleagues Doctors Ju Budagov, Glagolev V, Davydov Yu, Artikov A, Chokheli D for their support this work.

References

1. Kharzheev Yu N (2015) Scintillation Counters in Modern High-Energy Physics Experiments. Phy Particles Nuclei 46: 678-728.
2. Akimov Yu K (2014) Photon Methods of Radiation Detection, Dubna, Russian.
3. Bartoszek, Barnes LE, Miller JP, Mott J, Palladino A, et al. Mu2e Technical Design Report. arXiv: 1501.05241.
4. Bugg W, Eremenko Yu, Vasilyev S (2014) Large Scintillator panel with WLS fiber readout: Optimization of components. Nucl Instrum Meth A 758: 91-96.
5. Artikov A, Baranov V, Budagov Yu, Chokheli D, Davydov Yu, et al. (2016) Optimization of the light yield by injecting an optical filler into the co-extruded hole of the plastic scintillation bar. J Instrum 11: T05003.
6. Artikov A, Baranov V, Budagov J, Chokheli D, Davydov Yu, et al. (2016) The light yield of a long scintillation strip with WLS fiber embedded into the co-extruded hole. Report on the International conference at Minsk.
7. Abazov VM, Fox H, Abbott M, Abolins M (2005) Upgraded D0 detector. Nucl Instrum Meth A 552: 372-398.
8. Ask S, Barrillon P, Braem A, Vorobelet V (2006) Luminosity measurement at ATLAS - development, construction and test of scintillating fiber prototype detector. Nucl Instrum Meth A568: 588-600.
9. Cohen EO, Eli P, Yair S, Nikolay P (2016) Development of Sc.-fiber beam detector for MUSE. Nucl Instrum Meth A 815: 75-82.
10. Brown RM, Cockerill DJA (2012) Electromagnetic calorimeters. Nucl Instrum Meth A 666: 47-79.
11. Akchurin N, Wigmans R (2012) Hadron Calorimetry. Nucl Instrum Meth A 666: 80-97.
12. Chatrchyan S, Hmayakyan G, Khachatryan V, Sirunyan AM, Adam W (2008) CMS experiment at the CERN LHC. J Instrum 3: S08004.
13. Shopper A (2010) Overview of the LHCb calorimeter system Nucl Instrum Meth A 623: 219-221.
14. Aad G, Abat E, Abdallah J, Abdelalim AA, Abdesselam A, et al. (2008) The ATLAS experiment at the CERN Large Hadron Collider. J Instrum 3: S08003.
15. http://www.ihep.ru/scint/mold/product.htm
16. Allen J, Awes TC, Badalá A, Ward RM, (2010) Performance of prototype for the ALICE electromagnetic calorimeter. Nucl Instrum Meth A 615: 6-13.
17. Atoian GS, Britvich GI, Chernichenko SK, Dhawan S, Issakov VV, et al. (2008) An improved shashlyk calorimeter. Nucl Instrum Meth A 584: 291-303.
18. Anfimov N, Anosov V, Chirikov-Zorin I, Zhmurin PN, (2013) Shashlyk EM calorimeter prototype readout by MAPD with super high pixel density for COMPASS II. Nucl Instrum Meth A 718: 75-77.
19. Lee-Franzini J, Antonelli A, Wölfle S, Antonelli S (1995) KLOE electromagnetic calorimeter. Nucl Instrum Meth A 360: 201-205.
20. Nabb RMc, Blackburn J, Crnkovic JD, Hertzog DW, Kiburg B, et al. (2009) Tungsten/scintillating fiber electromagnetic calorimeter prototype for a high-rate muon (g-2) experiment. Nucl Instrum Meth A 602: 396-402.
21. Aldloff C, Basara L, Bigongiari G, Zhuang HL (2013) The AMS-02 lead-scintillating fibers calorimeter. Nucl Instrum Meth A 714: 147-154.
22. Casadei D, Bindi V, Carota N, Zichichi A, Castellini G, et al. (2002) The AMS-02 time of flight system. Nucl Phys B 113: 133-138.
23. Tomassetti N (2015) AMS-02 in space: physics results, overview, and challenges. Nucl Particle Phy Proceedings 650: 245-247.
24. Michael DG, Trevor J, Sousa A, Jensen D, Becker BR, et al. (2008) The magnetized steel and scintillator calorimeters of the MINOS experiment. Nucl Instrum Meth A 596: 190-228.
25. Acquafredda R, Adam T, Agafonova NYu, Zimmermann R (2009) The OPERA experiment in the CERN to Gran Sasso neutrino beam. 4: P04018.
26. Aliaga L, Bagby L, Baldin B, Ziemer B (2014) Design, calibration and performance of the MINERvA detector. Nucl Inst Meth A 743: 130.
27. Allan D, Andreopoulose C, Angelsene C, Barkeri GJ, Barr G, et al. (2013) The electromagnetic calorimeter for the T2K near detector ND280. IOP Publishing Ltd.
28. Deiters K, Ingram Q, Musienko Y, Nicol S, Patel P, et al. (2000) Properties of the avalanche photodiodes for the CMS electromagnetic calorimeters. Nucl Instrum Meth A 453: 223-226.
29. Musienko Y, (2009) Advances in multipixel Geiger-mode avalanche photodiodes. Nucl Instrum Meth A 598: 213-216.
30. Dolgoshein B, Mirzoyan R, Popova E, Zhukov A, Ilyin A, et al. (2012) Large area UV SiPMs with extremely low cross-talk. Nucl Instrum Meth A 295: 40-43.
31. Adloff C, Karyotakis Y, Repond J, Brandt A, Brown H, et al. (2010) Construction and commissioning of the CALICE analog hadron calorimeter prototype. J Instrum 5: P05004.
32. Garutti E (2011) Silicon Photomultipliers for High Energy Physics Detectors. J Inst 6: 1-14.
33. Danilov M (2007) Scintillator tile hadron calorimeter with novel SiPM readout. Nucl Instrum Meth A 581: 451-456.
34. Francis K, Repond J, Schlereth J, Smith J, Xia L, et al. (2014) Performance of the first prototype of the CALICE scintillator strip electromagnetic calorimeter. Nucl Instr Meth A 763: 278.
35. Abraamyan Kh, Afanasiev SV, Alfeev VS, Anfimov N, Arkhipkin D, et al. (2011) The MPD detector at the NICA heavy-ion collider at JINR. Nucl Instrum Meth A 628: 99-102.
36. Bross Alan D (2012) Application for Large Solid Scintillator Detectors in Neutrino and Particle Astrophysics. Nuclear Physics B 229: 363-367.
37. Stoykov A, Scheuermamm R, Sedlak S, (2012) A time resolution study with a plastic scintillator read out by a Geiger-mode avalanche photodiode. Nucl Instrum Meth A 695: 202-205.
38. Cattaneo PW, Gerone M, Gatti F, Nishimura M, Ootani W, et al. (2014) Development of the high precision timing counter based on plastic scintillator with SiPM readout. 61: 2657-2666.